



## Review

# PI-RADS version 2.1: one small step for prostate MRI



T. Barrett<sup>a,\*</sup>, A. Rajesh<sup>b</sup>, A.B. Rosenkrantz<sup>c</sup>, P.L. Choyke<sup>d</sup>, B. Turkbey<sup>d</sup>

<sup>a</sup> Department of Radiology, Addenbrooke's Hospital and the University of Cambridge, Cambridge CB2 0QQ, UK

<sup>b</sup> University Hospitals of Leicester NHS Trust, Leicester General Hospital, Radiology Department, Gwendolen Road, Leicester LE5 4PW, UK

<sup>c</sup> Department of Radiology, NYU School of Medicine, NYU Langone Medical Center, 660 1st Ave, Third Floor, New York, NY 10016, USA

<sup>d</sup> Molecular Imaging Program, Center for Cancer Research, National Cancer Institute, Bethesda, MD 20892, USA

Multiparametric (mp) prostate magnetic resonance imaging (MRI) is playing an increasingly prominent role in the diagnostic work-up of patients with suspected prostate cancer. Performing mpMRI before biopsy offers several advantages including biopsy avoidance under certain clinical circumstances and targeting biopsy of suspicious lesions to enable the correct diagnosis. The success of the technique is heavily dependent on high-quality image acquisition, interpretation, and report communication, all areas addressed by previous versions of the Prostate Imaging-Reporting and Data System (PI-RADS) recommendations. Numerous studies have validated the approach, but the widespread adoption of PI-RADS version 2 has also highlighted inconsistencies and limitations, particularly relating to interobserver variability for evaluation of the transition zone. These limitations are addressed in the recently released version 2.1. In this article, we highlight the key changes proposed in PI-RADS v2.1 and explore the background reasoning and evidence for the recommendations.

© 2019 The Royal College of Radiologists. Published by Elsevier Ltd. All rights reserved.

## Introduction

Prostate cancer is the most common male non-cutaneous cancer, with an overall mortality rate of the disease now exceeding that of breast cancer in the UK.<sup>1,2</sup> Recent level 1a literature evidence supports the use of multiparametric (mp) magnetic resonance imaging (MRI) for the diagnosis of tumours, showing an incremental improvement in detection compared to systematic non-targeted transrectal prostatic biopsy.<sup>3–6</sup> Indeed, in England, the use of MRI pre-biopsy in

men presenting with a suspicion of prostate cancer has increased from 55% in 2016 to 80% in 2018.<sup>7</sup>

The high incidence of the disease necessitates widespread adoption of prostate MRI; it cannot remain the preserve of tertiary referral centres. To ensure successful outcomes, the images need to be of sufficient quality and must be reported to a high level. These points are highlighted by the improved outcomes from single-site, experienced centres<sup>6</sup> compared to multicentre studies, which incorporate differing MRI protocols and variable levels of radiologist experience.<sup>3–5</sup> The Prostate Imaging-Reporting and Data System (PI-RADS) recommendations have been developed with the aim of addressing these issues by standardising the acquisition, interpretation, and reporting of prostate mpMRI examinations.

\* Guarantor and correspondent: T. Barrett, Department of Radiology, Addenbrooke's Hospital and the University of Cambridge, Cambridge, CB2 0QQ, UK. Tel.: +(44) 01223 336895; fax: +(44) 01223 330915.

E-mail address: [tristan.barrett@addenbrookes.nhs.uk](mailto:tristan.barrett@addenbrookes.nhs.uk) (T. Barrett).

## Evolution not revolution

The original 2012 European Society of Urogenital Radiology (ESUR) prostate MRI recommendations (retrospectively termed PI-RADS version 1) focused on image acquisition, providing different protocols for detection, staging, and node/bone assessment, and setting minimal and optimal parameters<sup>8</sup>; however, the system did not fully describe the process of deriving an overall assessment category, leading to variable applications in practice.<sup>9</sup> PI-RADS version 2 (v2) incorporated key advances in both acquisition, with a uniform protocol recommended and no longer including magnetic resonance spectroscopy, and interpretation using a prescriptive algorithm provided for deriving a five-point final score based on zone-specific dominant sequences.<sup>10</sup> Version 2 was intended as a “living” web-based document that could evolve with clinical practice. Indeed, since its original online publication in 2015, the document has seen the subsequent additions of an image atlas and introduction of report templates.

PI-RADS v2 has seen a broad uptake, with several studies validating the scoring system<sup>11–13</sup>; however, experience has also highlighted ambiguities in the scoring<sup>14,15</sup> and limitations in relation to inter-reader reproducibility.<sup>16,17</sup> Version 2.1 recommends several minor adjustments aimed at simplifying assessment and reducing inter-reader variability, without changing the overall scope or principles of the original system.<sup>18</sup> For these reasons, the document constitutes v2.1 rather than “version 3”. Herein, we highlight the key changes proposed in PI-RADS v2.1 and explore the background reasoning and evidence for the recommendations.

## MRI acquisition

The definition of mpMRI remains that of T2-weighted (T2W) imaging, diffusion-weighted imaging (DWI), and dynamic contrast-enhanced (DCE) sequences. Version 2.1 does not recommend biparametric (bp)MRI use, but acknowledges the growing investigation of bpMRI,<sup>19–21</sup> which may offer additional ancillary benefits such as avoidance of adverse effects of gadolinium and reduced examination time and cost, which may encourage greater uptake of MRI.

Issues of patient preparation have not been revisited following a lack of consensus in version 2. It should be noted that there is some emerging evidence in this field, particularly in relation to refraining from ejaculation,<sup>22,23</sup> for administration of antispasmodics,<sup>24,25</sup> and for bowel cleansing.<sup>26–28</sup>

### T2W imaging

T2W imaging remains the key sequence for staging disease and assessing lesions in the transition zone (TZ). High-resolution, small field-of-view axial images enable evaluation of lesion encapsulation in the TZ, but may be limited by partial voluming, necessitating assessment in additional planes. In version 2, the recommendation was to perform T2W imaging in the axial, sagittal, and coronal planes;

however, PI-RADS v2.1 now states that T2W images should be obtained in the axial plane and a minimum of one additional orthogonal plane. A preference for the choice of secondary plane is not explicitly stated; however, subsequent guidance on gland volume calculation describes measurement on the sagittal plane. The plane of axial acquisition can be acquired either in a true axial plane to the patient, as recommended in current UK consensus documentation for reproducibility purposes,<sup>29</sup> or in an oblique axial plane perpendicular to the long axis of the prostate.<sup>30</sup> An axial plane oriented orthogonal to the rectum and the posterior aspect of the prostate is not mentioned in v2.1, although this will better reflect the slice orientation of prostatectomy specimens,<sup>31</sup> this may be of limited additional benefit in clinical, non-research settings.

### DWI

Version 2 stated that the low b-value images should be acquired at 50–100 s/mm<sup>2</sup>, in order to avoid the perfusion/pseudo-diffusion effects at a b-value of 0 s/mm<sup>2</sup><sup>232–34</sup>; however, it is noted that the potential advantages of doing so have not subsequently been confirmed and that there may be technical challenges in meeting this requirement with certain equipment. Hence, the use of b=0 is now deemed acceptable. There has been further clarification in the definition of the maximum value from which to calculate the apparent diffusion coefficient (ADC) maps. It is now more strongly indicated that the ADC map should be calculated only using b-values up to 1,000 s/mm<sup>2</sup>, to avoid the kurtosis effects that occur at higher b-values and can impact ADC calculation.<sup>35,37</sup> Although a high b-value image ( $\geq 1,400$  s/mm<sup>2</sup>) is mandatory, this should be acquired separately or may be achieved by using calculated/synthetic images, generated by extrapolation from the acquired lower b-value data<sup>10</sup> (Fig 1).

### DCE MRI

In recognition of the widespread availability of three-dimensional (3D)-DCE sequences on current systems and the committee’s consensus that 3D confers signal: noise ratio (SNR) advantages over 2D-DCE, it is now stated that a 3D acquisition is the preferred option. High spatial resolution is advantageous for DCE to allow differentiation of periprostatic veins, which may provide false-positive high DWI signal<sup>38</sup> and can enable anatomical differentiation of the peripheral zone (PZ) and TZ when this may be unclear on T2W imaging at the apex due to partial voluming. Another benefit of high spatial resolution is evaluating for the more homogeneous enhancement typically seen in tumours and described in the TZ as being “sheet-like”, rather than a benign swirled or popcorn-like pattern.<sup>14</sup> The choice of temporal resolution involves a trade-off in spatial resolution, and the previous recommendations of  $\leq 10$  seconds (with  $< 7$  seconds preferred) risked compromising image quality on some scanners, therefore version 2.1 advises that temporal resolution can be increased up to 15 seconds. Theoretically a longer temporal resolution could risk

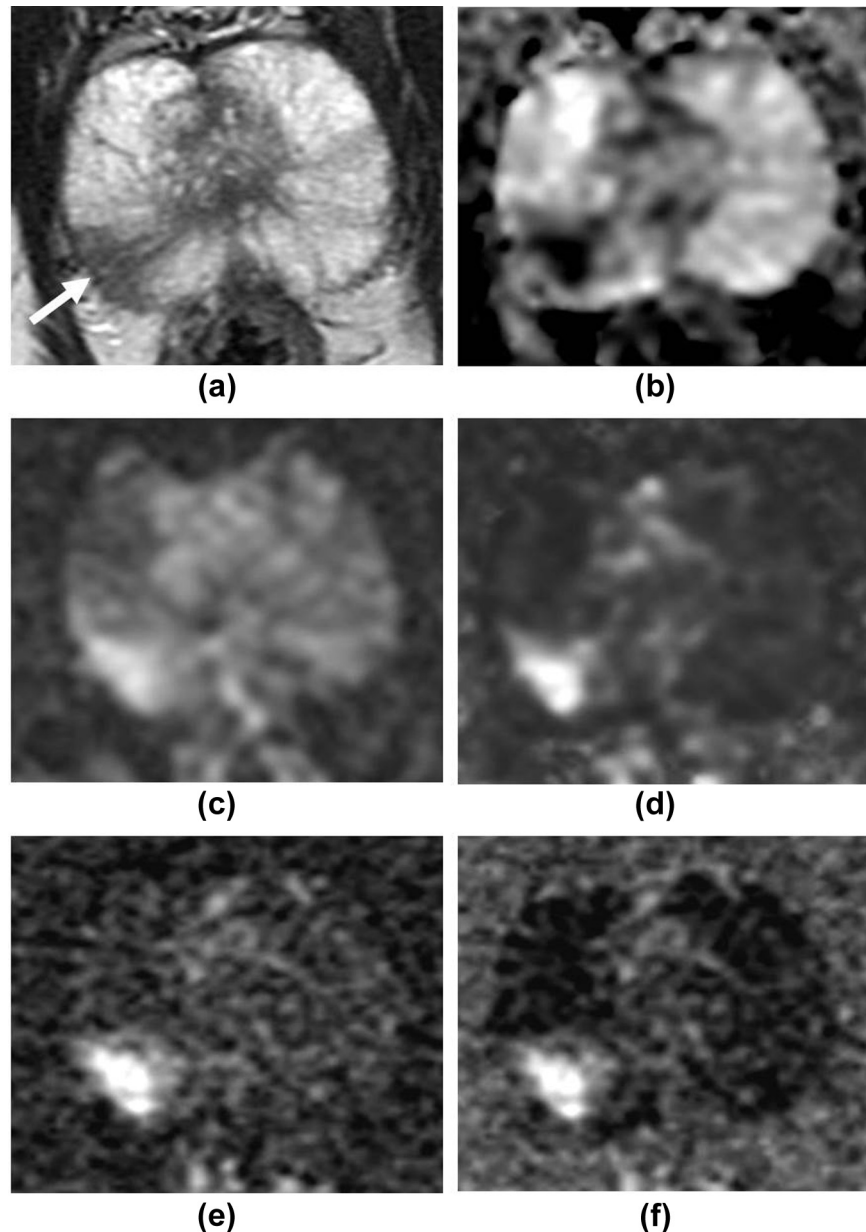


**Figure 1** Benefit of synthetic b-values in a 61-year-old biopsy-naive man with a PSA of 8.29 ng/ml. (a,b) Axial T2-weighted image (a) shows a wedge-shaped area of low signal in the right mid-gland laterally (arrow), with restricted diffusion on ADC maps (b). (c) Acquired large field of view (FOV)  $b=1,000$  image shows increased signal in this region, but with limited conspicuity over background normal signal; this in isolation would be PI-RADS score 3 for DWI. (d) Synthetic  $b=1,500$  image calculated from large FOV  $b=50/750/1,000$  image shows reduced signal in the normal prostate with high conspicuity of the lesion, confirming PI-RADS score 4 for DWI. (e,f) Acquired small FOV  $b=2,000$  image (e) shows the lesion well, with further increased conspicuity seen in the synthetic  $b=2,500$  image (f). Targeted transperineal biopsy showed Gleason 3+4=7 in all four cores, with 9 mm maximum tumour length.

missing focal early enhancement of a PZ lesion in a gland with background inflammation/prostatitis; however, recent studies suggest that lesion detection is not compromised by extending timing beyond 10 seconds,<sup>39</sup> and even up to 15 seconds.<sup>40</sup>

#### *bpMRI*

In PI-RADS version 2, DCE only affected the scoring of PZ lesions receiving a score of 3 on DWI, and had no

formal role in TZ lesion scoring. Version 2 also provided a supplementary scoring system using T2W imaging for DWI score 3 lesions in the PZ in the absence of DCE. To further clarify the value of DCE, a number of studies have looked at the merits of bpMRI, using diagnostic T2W and DWI alone. Initial studies were retrospective, often including mixed patient populations, and in some cases, excluded patients with hip replacements or significant DWI artefact, where DCE is of known benefit, or used surgical series with the inherent likelihood of including

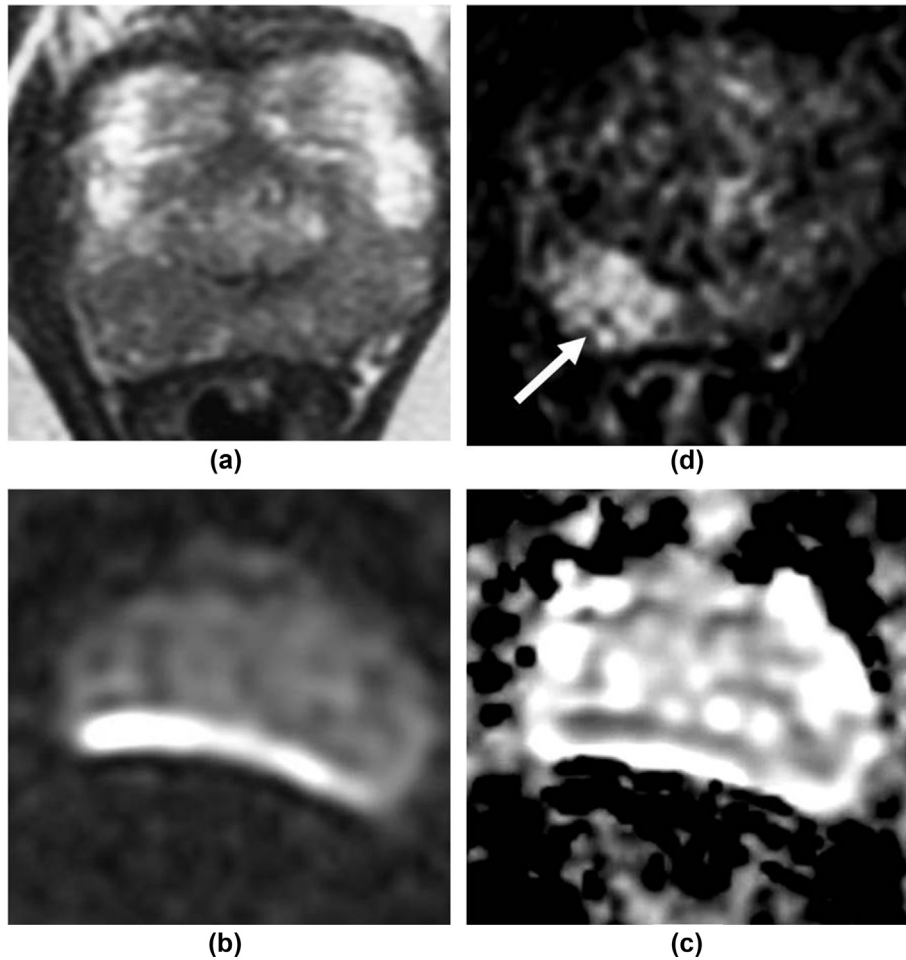


**Figure 2** Advantage of DCE in DWI failure in a 60-year-old biopsy-naive man with a PSA of 4.87 ng/ml. (a) Geographical low T2 signal bilaterally at the apex in the posterior PZ. Distortion artefact due to rectal gas affects b-value (b) and ADC maps (c) making these uninterpretable. (d) Focal early enhancement in the right apex PZ (arrow) makes this suspicious for tumour. Targeted transperineal biopsy of the right apex showed Gleason 4+3 disease.

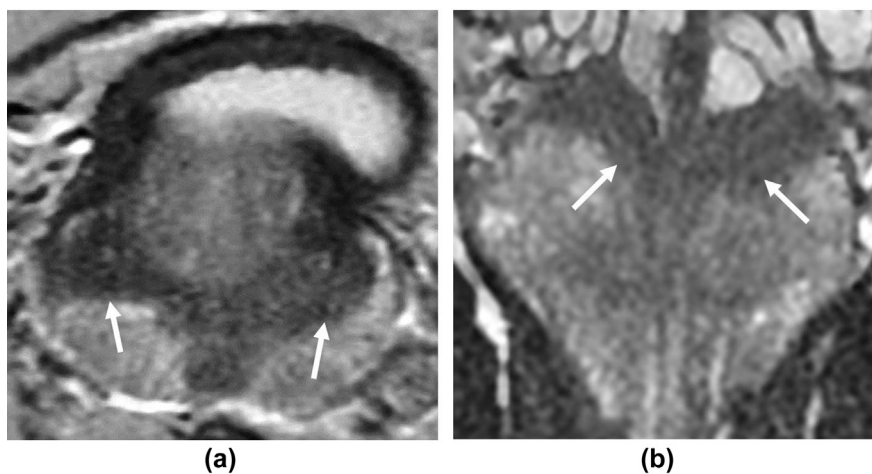


**Figure 3** Normal CZ appearances. (a,b) Normal CZ at the base level identified as bilateral symmetrical low T2 signal intensity tissue surrounding the ejaculatory ducts (arrows), located posterior to the TZ and the urethra on axial imaging (a), and coursing medially to join with the urethra at the level of the verumontanum, often better appreciated on coronal imaging (b).

larger lesions, which are more conspicuous on all sequences.<sup>21,41,42</sup> Subsequent prospective studies have also supported the efficacy of a biparametric approach<sup>19,20</sup>; however, the PI-RADS Steering Committee has continued concerns regarding the broad adoption of bpMRI and emphasises that the utility of bpMRI relies on T2W and DWI that is of high quality and artefact-free, which may not always be the case, particularly in the absence of an endorectal coil<sup>27</sup> (Fig 2). Although lower volume centres may particularly benefit from the use of DCE to help overcome any issues with T2W or DWI image quality<sup>43</sup> and to aid the less experienced readers,<sup>44</sup> it is paradoxical that these centres are the ones more likely to employ a biparametric approach.<sup>45</sup> A further implication is the potential for category shift, with a biparametric approach potentially resulting in a higher number of PI-RADS 3 and fewer score 4 lesions, which may have implications for score-based management pathways.<sup>15</sup> The committee also notes that no head-to-head comparisons have been performed, and studies to date have been single-centre studies with experienced readers. Thus, future multi-centre studies with readers of mixed experience are encouraged to further explore bpMRI.

The consistently high sensitivity and negative predictive value (NPV), but more variable specificity of prostate MRI suggests that it performs better as a “rule out” rather than a “rule in” test for clinically significant prostate cancer (csPCa).<sup>3,15,46,47</sup> Indeed, this is of particular benefit when applied to clinical practice and the potential to avoid biopsy in low-risk patients with a negative MRI; thus, the investigation should be performed to its optimal level. DCE has been shown to further increase sensitivity for lesion detection in both the PZ and TZ,<sup>30,48,49</sup> particularly in men with lower prostate-specific antigen (PSA) levels (<10 ng/ml),<sup>50</sup> and for less experienced readers,<sup>44</sup> and can potentially serve as a “safety net” for detection of lesions missed on initial review of other sequences. Furthermore, in circumstances where DWI fails and no DCE has been performed, PI-RADS states that the MRI assessment should be limited to staging alone. DCE also remains essential in the assessment of local recurrence following prior radical treatment or focal therapy (although PI-RADS assessment criteria explicitly do not currently apply to these cohorts). The committee suggests that bpMRI be reserved for select clinical indications;

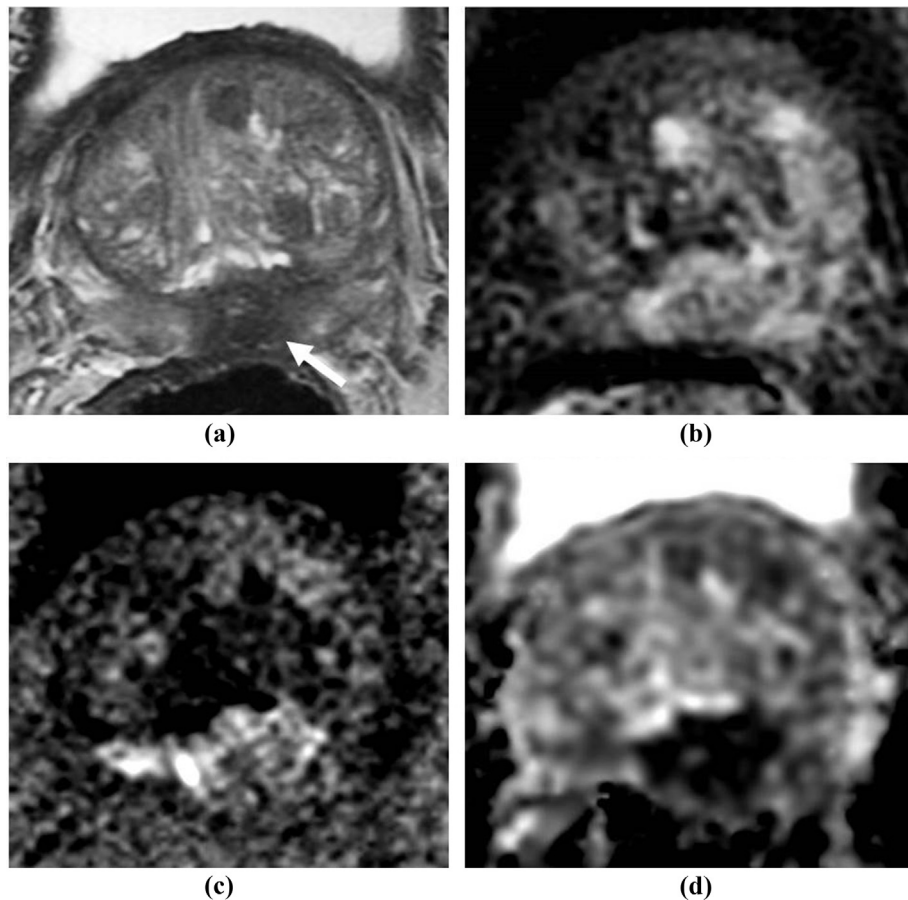


**Figure 4** CZ tumour in a 73-year-old patient with a PSA of 8.87 ng/ml. (a) Low T2 signal with minor asymmetry at the base, within the central zone (arrow). (b) Focal early enhancement on DCE. (c,d) Marked restricted diffusion within this area, particularly to the left of midline. Reported as high probability for CZ tumour, with additional direct extension into the seminal vesicles. Biopsy of this region showed Gleason 4+5 disease with core involvement up to 19 mm.

however, rather than endorsing scenarios where bpMRI could be utilised, v2.1 identifies circumstances in which mpMRI is the preferred option, along with the suggestion that mpMRI be used when the clinical priority is not to miss any significant cancer. The latter proviso may be of particular relevance to biopsy-naive men in whom prostate MRI may be the only test performed (aside from screening PSA) and, if negative, used as a means to avoid biopsy. This justifies the additional cost of contrast medium and the opportunity to perform the test to its optimal diagnostic potential; thus, DCE remains an integral component of prostate MRI.

## Interpretation

The interpretation and scoring system employed in v2 applied to lesions arising from the PZ or TZ; however, some areas do not fit this binary definition, for instance, the central zone (CZ), anterior fibromuscular stroma (AFMS), or at the PZ/TZ interface where the region of lesion origin is uncertain. This has been a highlighted weakness of PI-RADS and partially explains the UK preference for a Likert scoring

system<sup>29</sup>; however, advice is now offered for these areas in v2.1. Nonetheless, separate scoring criteria are not provided for these regions, and if no abnormality is present in the CZ or AFMS, they do not need to be reported separately. Additional clarification is proposed for the definition of a negative DCE score, and minor changes have been made to the scoring used systems in the TZ, and for DWI. Application of the PI-RADS scoring system remains explicitly for initial MRI assessment only, and not for assessment post-treatment. Criteria are not provided for determining whether a lesion on active surveillance has progressed between examinations.

## CZ

The CZ is a Wolffian duct derivate with similar histological features to those of the seminal vesicles, which, unlike the remaining prostatic tissue, derives from the urogenital sinus.<sup>51</sup> The normal CZ can be identified in up to 93% of MRI studies,<sup>52,53</sup> and is seen as low T2 signal intensity tissue surrounding the ejaculatory ducts, located posterior to the transition zone at prostatic base, and coursing medially to the urethra at the level of the

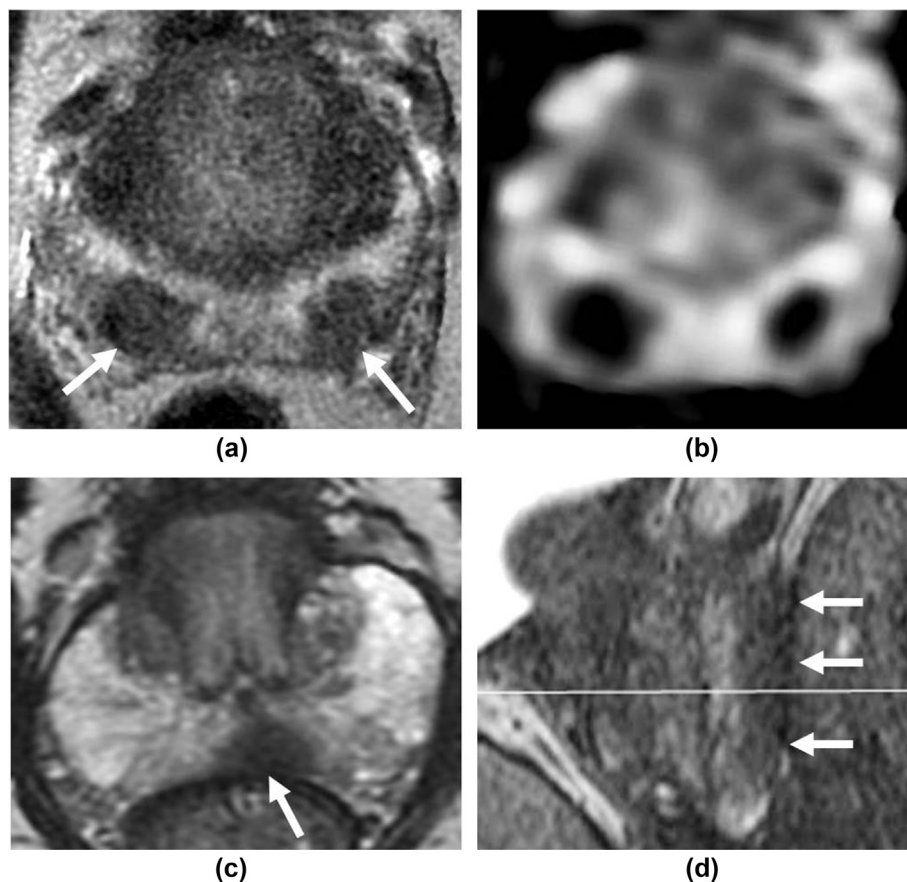


**Figure 5** “Pitfall of the pitfall” tumours. (a,b) Bilateral base level PZ tumours (arrows). Despite symmetric appearances, the lesions are within the PZ rather than central zone (a); with marked restricted diffusion noted on ADC maps (b). Bilateral tumours were confirmed on targeted biopsy and subsequent prostatectomy: Gleason 4+3 on right and 3+4 on left. (c,d) Tumour located medially within the left base/mid PZ, with mild asymmetry (c), and confirmed to pass below the level of the verumontanum on sagittal imaging (arrows in d), therefore not relating to the CZ; biopsy confirmed Gleason 4+3 tumour.

verumontanum, often better appreciated on coronal imaging<sup>54</sup> (Fig 3). Normal CZ can demonstrate mild increased signal intensity on b-value imaging, and typically has ADC values lower than normal PZ/TZ tissue and overlapping with tumour ADC values.<sup>55</sup> CZ tumours account for <5% of all prostatic cancer, but tend to be more aggressive, with a higher grade and increased incidence of extracapsular extension and seminal vesicle invasion,<sup>56</sup> making identification important. Key to assessment is the symmetrical appearance at the base level, compressed by the TZ posteriorly into a teardrop or “moustache” shape.<sup>36</sup> A CZ tumour is suspected when asymmetry is present or extension below the verumontanum is confirmed in multiple planes; however, a normal CZ can appear asymmetric in 18% of cases,<sup>52</sup> particularly in the setting of significant benign prostate hyperplasia (BPH). To identify CZ tumours, it can be useful to assess for presence of a “mass-like” change rather than simple asymmetry. DCE is also helpful for evaluation of the normal CZ, which typically demonstrates a type 1 (progressive) enhancement curve compared to CZ tumours, which demonstrate early enhancement and a type 3 (wash-out) curve<sup>53</sup> (Fig 4). Care has to be taken to avoid the “pitfall of a pitfall” when tumour mimics normal CZ anatomy, for example, bilateral basal PZ tumours manifesting in a similar fashion to the CZ<sup>36</sup> (Fig 5).

## AFMS

Lesions do not originate from the AFMS, but can arise from the adjacent PZ or TZ, or invade into the AFMS.<sup>57</sup> It is acknowledged that possible ambiguity of lesion zone of origin is a limitation of PI-RADS, and therefore, interpretation and application of the scoring system here has some inherently subjective components. Knowledge of the imaging appearances of the normal AFMS is of value: crescentic low T2 signal, no high signal on b-value imaging, mildly reduced ADC, and a type 1 (progressive enhancement) curve on DCE.<sup>58,59</sup> An easy way to remember these normal appearances is “low on all sequences”. Muscle within the bladder wall is a useful internal reference point for T2W signal intensity, with AFMS being iso- or hypointense, and tumour being mildly hyperintense. The close association of the AFMS to the TZ leads to a tendency to apply the TZ scoring system to this region, including the dominance of T2WI; however, DWI, especially the high b-value image, and DCE may be essential for evaluation of this region, particularly in cases with asymmetry or a bulky appearance on T2WI. Tumour will demonstrate focal high signal on the b-value image as well as early enhancement on DCE (Fig 6), in contradistinction to normal AFMS, which does not show true restricted diffusion, and demonstrates delayed enhancement due to its fibrous composition.

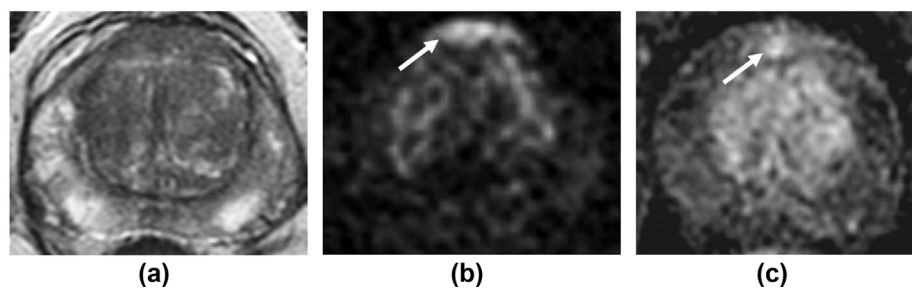


**Figure 6** Anterior tumour in a 65-year-old biopsy-naive man with a PSA of 6.5 ng/ml. (a) No clear abnormality demonstrated in the anterior gland on T2W imaging (the key sequence for the TZ). (b) Focal high signal on b=2,000 DWI suspicious for tumour (arrow), with focal early enhancement confirmed on DCE (c). Targeted biopsy confirmed Gleason 3+4 tumour.

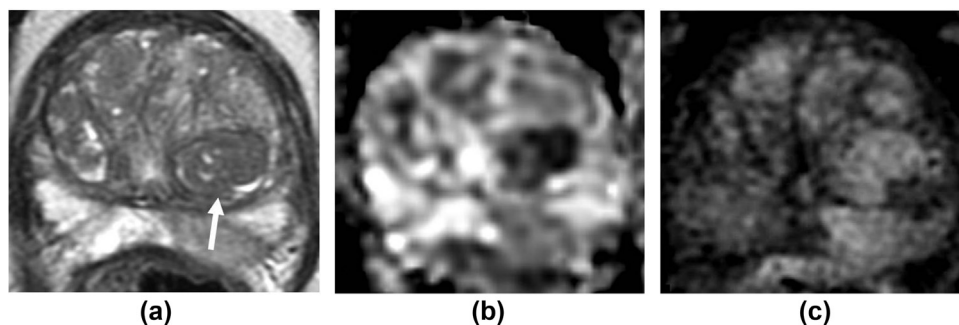


**Figure 7** New PI-RADS T2W imaging category 1 in the TZ. A 74-year-old man with a PSA of 16.04 ng/ml underwent systematic transrectal ultrasound (TRUS) biopsy, which showed one core Gleason 3+3 on the right side, and MRI for staging. (a) Fully encapsulated nodule in the left TZ (arrow) is of PI-RADS category 1 (previously, version 2 = category 2). Additional benign features include foci of high T2 signal within, consistent with microcysts (dilated hyperplastic acini), and posteriorly location. (b) Marked restricted diffusion on ADC maps, making this score 5 for DWI based on size. (c) Positive on DCE, with early enhancement. T2W imaging is the dominant sequence in the TZ; overall PI-RADS score 1.

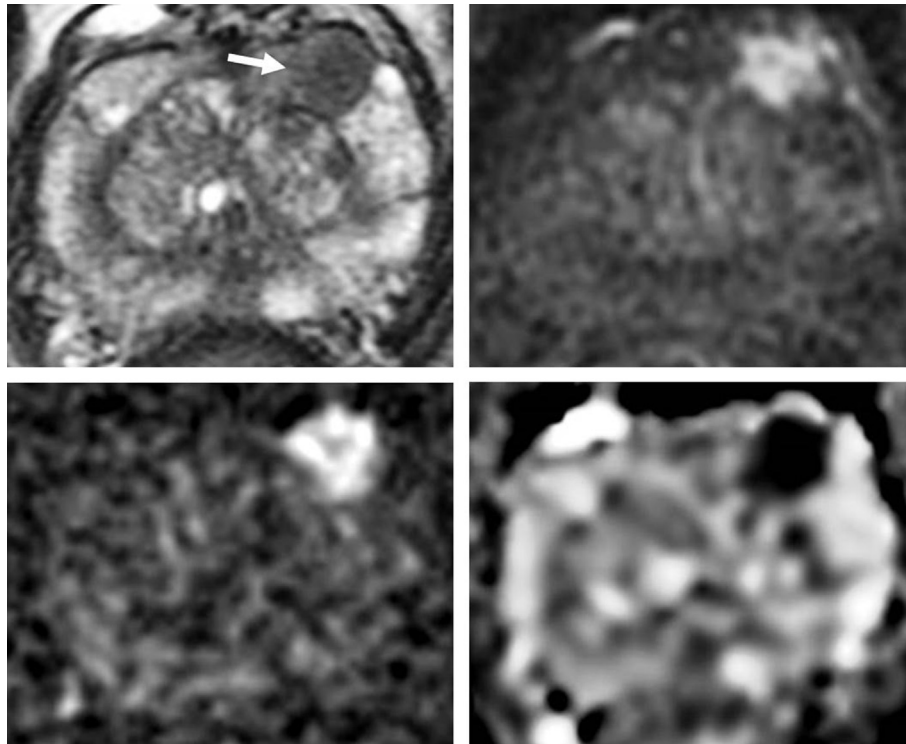


**Figure 8** Up-scoring T2 category 2 lesions with DWI in a 75-year-old biopsy-naive man with a PSA of 9.5 ng/ml. (a) Partly encapsulated homogeneous circumscribed nodule within the anterior mid TZ (arrow), PI-RADS score 2 on T2W imaging as an “atypical nodule”. (b) Focal early enhancement on DCE. (c,d) The nodule demonstrates marked restricted diffusion on b=2,000 (c) and ADC maps (d), PI-RADS score 4 on DWI. Overall PI-RADS v2.1 score 3. Targeted transperineal biopsy demonstrated Gleason 4+3 tumour in 2/3 cores, with all other background cores negative.

*Evaluation of the TZ*

The TZ is challenging to assess on all imaging sequences, typically containing hyperplastic nodules, areas of cystic change, and glandular and stromal components of mixed T2

**Table 1**  
Guidance for assignment of overall PIRADS-v2.1 score.

Peripheral zone			
DWI score (dominant sequence)	DCE score (secondary sequence)	T2W imaging score	Overall PIRADS-v2 score
1	Any	Any	1
2	Any	Any	2
3	- ve	Any	3
3	+ ve	Any	4
4	Any	Any	4
5	Any	Any	5
Transition zone			
T2W imaging score (dominant sequence)	DWI score (secondary sequence)	DCE score	Overall PIRADS-v2 score
1	Any	Any	1
2	≤ 3	Any	2
2	≥ 4	Any	3
3	≤ 4	Any	3
3	5	Any	4
4	Any	Any	4
5	Any	Any	5

NB peripheral zone scoring system remains unchanged from version 2.

**Table 2**  
PI-RADS scoring system changes in version 2.1.

Score criteria
<b>T2W for transition zone (TZ)</b>
1 Normal appearing TZ (rare) or a round, completely encapsulated “typical nodule”
2 A mostly encapsulated nodule OR a homogeneous circumscribed nodule without encapsulation (“atypical nodule”) OR a homogeneous mildly hypointense area between nodules
3 UNCHANGED [Heterogeneous signal intensity with obscured margins. Or other, not in categories 1/2 or 4/5]
4–5 UNCHANGED [Lenticular or non-circumscribed, homogeneous, moderately hypointense, either <1.5 cm (score 4), or ≥1.5 cm or features of ECE/invasive behaviour (score 5)]
<b>Diffusion-weighted Imaging</b>
1 UNCHANGED [No abnormality (i.e. normal) on ADC and high b-value DWI]
2 Linear/wedge shaped area that is hypointense on ADC and/or hyperintense on high b-value DWI
3 Focal area of hyperintensity on high b-value DWI and/or hypointense on ADC; may have marked change on b-value imaging or ADC, but not on both
4–5 UNCHANGED [Focal markedly hypointense on ADC and markedly hyperintense on high b-value DWI; either <1.5 cm (score 4), or ≥1.5 cm or features of ECE/invasive behaviour (score 5)]
<b>Dynamic contrast-enhanced MRI</b>
- No early or contemporaneous enhancement, or; diffuse multifocal enhancement NOT corresponding to a focal finding on T2W and/or DWI
+ UNCHANGED [Focal enhancement and earlier than adjacent normal tissue and corresponding to an abnormality on T2/DWI]

Scoring for T2-weighted imaging in the PZ remains unchanged and is not included. ECE, extra-capsular extension; BPH, benign prostatic hypertrophy; ADC, apparent diffusion co-efficient; DWI, diffusion-weighted imaging.

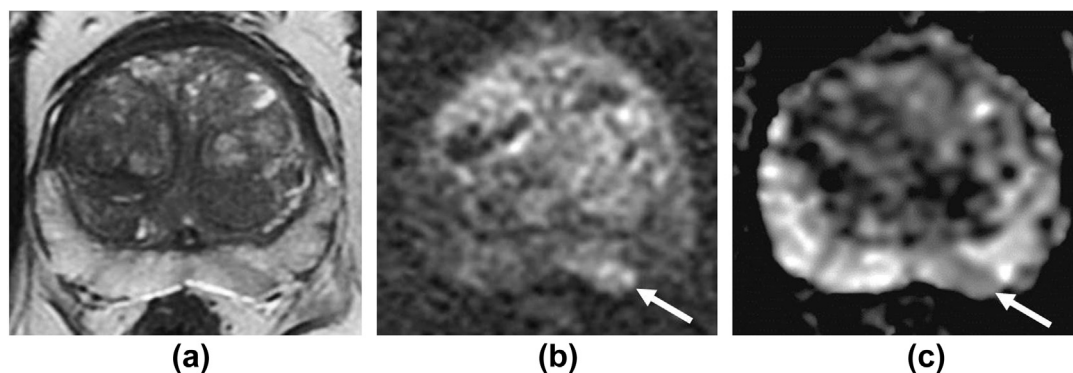


**Figure 9** New DWI category 2 in a 72-year-old patient, who was undergoing active surveillance for low-volume right-sided Gleason 3+3 disease. (a) Wedge-shaped area of intermediate T2 signal in the left mid PZ. (b,c) Wedge-shaped mild hyperintensity on  $b=2,000$  DWI (b; arrow) and low signal on ADC maps (c).

signal intensities. The morphological shape (lenticular) and marginal features (obscured) of lesions are key for T2 evaluation.<sup>60,61</sup> Thus, T2W imaging remains the dominant sequence and should be assessed in at least two planes. BPH is typical in the age demographic of men undergoing MRI for suspected prostate cancer, and this is now acknowledged in v2.1 by reclassifying classic-appearing BPH nodules (encapsulated) from previously PI-RADS score 2 to now PI-RADS score 1. Category 2 is now reserved for “atypical nodules,” which are almost, but not fully, encapsulated, or homogeneously circumscribed, or homogeneous mildly hypointense areas between nodules; the latter often scored as “3” using v2 criteria. Another useful feature for “score 2” nodules, not directly addressed in v2.1, but implied schematically, is the presence of microcysts within a nodule (Fig 7), which represent dilated hyperplastic acini and are a feature suggestive of benign change.<sup>62</sup>

The trend to down-score T2W imaging features is associated with an increased emphasis on DWI scoring in the TZ, reflecting the general importance of restricted diffusion within tumours. Version 2.1 emphasises the identification of areas in the TZ that are different from the background, wherein multiple nodules that demonstrate similar degrees of restricted diffusion are not scored. Conversely, areas

within or between nodules demonstrating more marked restricted diffusion than background TZ should be scored. Atypical TZ nodules (now PI-RADS score 2) can be upgraded to PI-RADS assessment category 3 if they have a DWI score of  $\geq 4$  (Fig 8), but importantly not with DWI score 3 (mild/moderate restricted diffusion; Table 1). A DWI score of 5 (i.e. size  $>15$  mm or invasive behaviour) rather than 4 is still required to up-score a T2W imaging category 3 to 4, a quirk of the system that is further accentuated by the new criteria for up-scoring T2W imaging score 2 lesions (only requiring DWI score 4); however, the latter change will be partially offset by the trend to down-score T2W imaging features in previous categories 2 and 3, and should lead to reduced inter-reader variability for lesions that are less conspicuous on T2W imaging but that display marked restricted diffusion.

#### Revision of DWI criteria

The DWI features of high probability (score 4–5) lesions, namely marked hyperintensity on high  $b$ -value imaging and marked low ADC, is well known to radiologists. Absolute ADC measurements do not form part of the scoring system. Version 2.1 addresses the definition of score 2 and 3

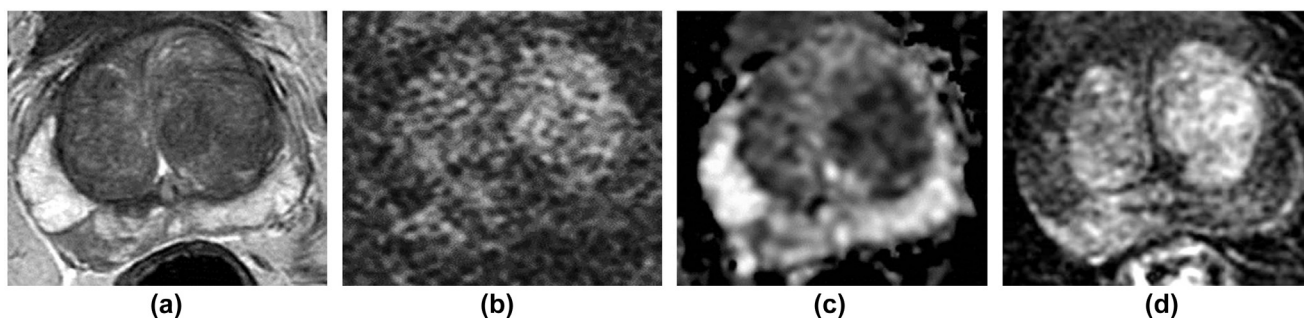


**Figure 10** Adjusted scoring for DWI category 2 in a 54-year-old biopsy-naive man, with a PSA of 5.72 ng/ml. (a) Wedge-shaped area of low T2 signal at the right base PZ; PI-RADS score 2. (b,c) DWI shows wedge-shaped mild hyperintensity on  $b=2,000$  (b) and mild hypointensity on ADC (c). PI-RADS version 2 this would be category 3 due to “focal mildly/moderately hypointense on ADC and isointense/mildly hyperintense on high  $b$ -value DWI”; however, on v2.1 this is category 2 due to “linear/wedge shaped area hypointense on ADC and/or hyperintense on high  $b$ -value DWI”. (d) Positive on DCE due to focal early enhancement matching a T2/DWI abnormality. DWI is the dominant sequence in the PZ, therefore the overall assessment category is PI-RADS 4 using v2, but PI-RADS score 2 with v2.1. Targeted biopsy was benign, with histological features of focal mild acute inflammation.

for DWI, which lacked clarity in v2, including the differentiation between “focal” and “indistinct” (Table 2). DWI category 2 is now defined as a linear/wedge-shaped area that is hyperintense on high b-value DWI and/or hypointense on ADC (Fig 9). This broadly mirrors the T2W scoring for PZ category 2, and is in part a reversion to the earlier recommendations of version 1, wherein DWI category 2 was defined as “diffuse, hyperintensity on  $\geq b=800$  image with low ADC; no focal features, however, linear, triangular, or geographical features are allowed”.<sup>8</sup> This should help to reduce the potential scoring of inflammation as score 3 on DWI, which in turn can be elevated to an overall PI-RADS category 4 if showing associated focal early enhancement (Fig 10). Score 3 is now defined as a focal area of hyperintensity on high b-value DWI and/or hypointense on ADC; this category may have marked change on b-value imaging or ADC, but not on both. The term “marked” as applied to categories 3–5 is now clearly defined as “a more pronounced signal change than any other focus in the same zone.”

#### Clarification of negative DCE scoring

The definition of positive findings on DCE is unchanged; however, the features of a negative score on DCE have been modified to help reduce over-calling and improve inter-reader reproducibility (Table 2). The definition is generally opposite to that of positive DCE, but also includes diffuse or multifocal enhancement, more typically associated with inflammatory change.

#### MRI reporting

A structured report remains the preferred format, with recent studies supporting this as a means to improve consistency and to ensure report completeness.<sup>63–65</sup> Since the original publication of v2, there have been the online additions of example report templates and an imaging atlas. The template suggests including a statement of PI-RADS protocol compliance, clinical information including PSA density, a comment on image quality, and to report findings at both a lesion and patient (overall) level.

There is increasing evidence for the use of PSA density as a clinical biomarker, with a threshold of 0.15 ng/ml/ml proving a useful aid to the clinical decision-making process.<sup>66–68</sup> As such, reporting of the gland volume is a key component of prostate MRI studies. This can be performed either by segmentation software or triplanar measurements using an ellipsoid formula. In a change to version 2, v2.1 recommends taking the maximum anteroposterior (AP) measurement from the mid-sagittal rather than axial T2 image, with the maximum transverse diameter still taken from the axial plane. The change will avoid variations in AP measurements that may relate to differences in the choice of axial plane, and ensure a more uniform measurement is acquired perpendicular to the long axis of the prostate.

The sector map used for lesion localisation has added two additional sectors to the base level of the PZ (right and left posterior PZ medial: PZpm). This brings the overall total

to 41 sectors, incorporating the 38 prostatic sectors, plus two for the seminal vesicles and one for the membranous urethra. The 38 prostatic sectors build on the earlier

**Table 3**

Summary of key changes made for PIRADS-v2.1.

- Format and scope
  - Scope remains for initial MRI assessment, not for assessment post-treatment
  - Recommends several minor adjustments aimed at simplifying assessment, without changing the overall categorisation framework, thus v2.1 rather than “version 3”
- MRI acquisition
  - T2W images to be obtained in the axial plane and a minimum of one additional orthogonal plane
  - Axial plane can be true axial to the patient or in an oblique axial plane matching the long axis of the prostate
  - Lowering of the acquired low b-value range to 0–100 s/mm<sup>2</sup> (50–100 s/mm<sup>2</sup> remains preferred)
  - The maximum high b-value for ADC map calculation is  $\leq 1,000$  s/mm<sup>2</sup>
  - High b-value DWI image of 1,400–2,000 s/mm<sup>2</sup> should be acquired separately, or may be generated by extrapolation from acquired lower b-value data
  - DCE is still recommended, although biparametric MRI is acknowledged
  - DCE 3D T1W GRE is preferred over 2D acquisitions
  - DCE temporal resolution increased to  $\leq 15$  s
- Interpretation
  - Guidance given for assessment of the CZ and AFMS. If no abnormality is present, they do not need to be reported separately
  - Tumours within the AFMS may arise from the PZ or TZ and judgement may be required as to which scoring system is applied.
  - The normal AFMS appears as “low on all sequences”
  - TZ assessment: increased emphasis on DWI features, including distinction from background TZ
  - Atypical TZ nodules on T2W imaging (score 2) are upgraded to category 3 if they have a DWI score of  $\geq 4$ . Presence of T2 hyperintense “microcysts” can help imply benignity
  - Definitions for DWI scores 2 and 3 have been revised; scores 1, 4, 5 remain unaltered from v2
  - DWI “marked” change as applied to scored 3–5 is defined as “a more pronounced signal change than any other focus in the same zone”
  - Negative DCE now more clearly defined (“positive” DCE definition is unchanged)
- Reporting
  - Structured reports still recommended. Example report templates are now provided on-line
  - The maximum AP prostate measurement should be taken from the mid-sagittal T2W image rather than axial T2
  - Sector maps consist of 38 prostatic regions (41 in total), an increase of two relating to the right and left posterior medial PZ
  - Sector map AFMS abbreviation change from “AS” to “AFS”

MRI, magnetic resonance imaging; T2W, T2-weighted; ADC, apparent diffusion coefficient; DWI, diffusion-weighted imaging; DCE, dynamic contrast-enhanced; 3D, three-dimensional; 2D, two-dimensional; GRE, gradient echo; CZ, central zone; AFMS, anterior fibromuscular stoma; PZ, peripheral zone; TZ, transition zone.

increase from 27 in version 1 to 36 in v2. Another minor change in the sector map is the anterior fibromuscular stroma abbreviation change from “AS” to “AFS”, which may avoid confusion with the standard abbreviation of “AS” used for active surveillance. Although the sector locations are a useful means of simplifying and standardising the message of lesion location to the end user, the inter-reader exact agreement for defining sectors has been shown to be low at 21.2%, with agreement on defining the same level of disease (i.e., apex, mid, base) only 61.4%.<sup>69</sup> This needs to be recognised as a source of potential error when a cognitive approach is taken to targeted biopsy.

## Summary

PI-RADS version 2 has been widely adopted and tested in clinical practice, with experience highlighting areas of ambiguity, poor performance, and reduced inter-reader variability. Version 2.1 makes several minor modifications aimed at addressing these issues and simplifying the scoring system without changing the overall framework for acquisition or interpretation using the principles of the dominant sequence paradigm (Table 3). Although bpMRI is now acknowledged, concerns are noted, and mpMRI remains advised in a range of scenarios. PI-RADS remains an assessment based on image features alone; however, other clinical factors may also, appropriately influence decisions to biopsy or not. As with prior versions, further research is encouraged to assess the accuracy, reproducibility, and interobserver agreement of v2.1 and to identify any improvements that may aid in the evolution of version 3.

## Conflict of interest

The authors declare no conflict of interest.

## Acknowledgements

T.B. is supported by the Cancer Research UK and Engineering and Physical Sciences Research Council Imaging Centre in Cambridge and Manchester and the NIHR Biomedical Research Centre. A.R. receives royalties from Thieme Medical Publishers.

## References

1. Siegel RL, Miller KD, Jemal A. Cancer statistics, 2017. *CA Cancer J Clin* 2017;**67**(1):7–30.
2. Cancer Research UK. Prostate cancer mortality statistics. Available at: <http://www.cancerresearchuk.org/health-professional/cancer-statistics/statistics-by-cancer-type/prostate-cancer/mortality>. [Accessed 2 April 2019].
3. Ahmed HU, El-Shater Bosaily A, Brown LC, et al. Diagnostic accuracy of multi-parametric MRI and TRUS biopsy in prostate cancer (PROMIS): a paired validating confirmatory study. *Lancet* 2017;**389**:815–22.
4. Kasivisvanathan V, Rannikko AS, Borghi M, et al. MRI-targeted or standard biopsy for prostate-cancer diagnosis. *N Engl J Med* 2018;**378**:1767–77.
5. Rouvière O, Puech P, Renard-Penna R, et al. Use of prostate systematic and targeted biopsy on the basis of multiparametric MRI in biopsy-naïve patients (MRI-FIRST): a prospective, multicentre, paired diagnostic study. *Lancet Oncol* 2019;**20**(1):100–9. [https://doi.org/10.1016/S1470-2045\(18\)30569-2](https://doi.org/10.1016/S1470-2045(18)30569-2).
6. van der Leest M, Cornel E, Israel B, et al. Head-to-head comparison of transrectal ultrasound-guided prostate biopsy versus multiparametric prostate resonance imaging with subsequent magnetic resonance-guided biopsy in biopsy-naïve men with elevated prostate-specific antigen: a large prospective multicenter clinical study. *Eur Urol* 2018 Nov 23;(18):30880–7. <https://doi.org/10.1016/j.eururo.2018.11.023> [Epub ahead of print]pii: S0302-2838.
7. NPCA. Annual report. 2018 <https://www.npca.org.uk/content/uploads/2019/02/NPCA-Annual-Report-2018.pdf>. [Accessed 2 April 2019].
8. Barentsz JO, Richenberg J, Clements R, et al. ESUR prostate MR guidelines 2012. *Eur Radiol* 2012;**22**(4):746–57.
9. Richenberg JL. PI-RADS: past, present and future. *Clin Radiol* 2016;**71**(1):23–4.
10. Weinreb JC, Barentsz JO, Choyke PL, et al. PI-RADS prostate imaging – reporting and data system: 2015, version 2. *Eur Urol* 2016;**69**(1):16–40.
11. Seo JW, Shin SJ, Taik Oh Y, et al. PI-RADS version 2: detection of clinically significant cancer in patients with biopsy Gleason score 6 prostate cancer. *AJR Am J Roentgenol* 2017;**209**(1):W1–9.
12. Greer MD, Shih JH, Lay N, et al. Validation of the dominant sequence paradigm and role of dynamic contrast-enhanced imaging in PI-RADS version 2. *Radiology* 2017;**285**(3):859–69.
13. Mehralivand S, Bednarova S, Shih JH, et al. Prospective evaluation of prostate imaging reporting and data system, version 2 using the international society of urological pathology prostate cancer grade group system. *J Urol* 2017;**198**(3):583–90.
14. Rosenkrantz AB, Babb JS, Taneja SS, et al. Proposed adjustments to PI-RADS version 2 decision rules: impact on prostate cancer detection. *Radiology* 2017;**283**(1):119–29.
15. Padhani AR, Weinreb J, Rosenkrantz AB, et al. Prostate imaging-reporting and data system steering committee: PI-RADS v2 status update and future directions. *Eur Urol* 2019;**75**(3):385–96.
16. Urysko AS, Bittencourt LK, Bullen JA, et al. Accuracy and interobserver agreement for Prostate Imaging Reporting and Data System, version 2, for the characterization of lesions identified on multiparametric MRI of the prostate. *AJR Am J Roentgenol* 2017;**209**(2):339–49.
17. Greer MD, Brown AM, Shih JH, et al. Accuracy and agreement of PIRADSV2 for prostate cancer mpMRI: a multireader study. *J Magn Reson Imaging* 2017;**45**(2):579–85.
18. Turkbey B, Rosenkrantz AB, Haider MA, et al. Prostate imaging reporting and data system version 2.1: 2019 update of prostate imaging reporting and data system version 2. *Eur Urol* 2019 Mar 18 <https://doi.org/10.1016/j.eururo.2019.02.033>.
19. Boesen L, Nørgaard N, Løgager V, et al. Assessment of the diagnostic accuracy of biparametric magnetic resonance imaging for prostate cancer in biopsy-naïve men: the Biparametric MRI for Detection of Prostate Cancer (BIDOC) Study. *JAMA Netw Open* 2018;**1**(2):e180219.
20. Jambor I, Bostrom PJ, Taimen P, et al. Novel biparametric MRI and targeted biopsy improves risk stratification in men with a clinical suspicion of prostate cancer (IMPROD Trial). *J Magn Reson Imaging* 2017;**46**(4):1089–95.
21. Kuhl CK, Bruhn R, Krämer N, et al. Abbreviated biparametric prostate MR imaging in men with elevated prostate-specific antigen. *Radiology* 2017;**285**(2):493–505.
22. Barrett T, Tanner J, Gill AB, et al. The longitudinal effect of ejaculation on seminal vesicle fluid volume and whole-prostate ADC as measured on prostate MRI. *Eur Radiol* 2017;**27**(12):5236–43.
23. Kabakus IM, Borofsky S, Mertan FV, et al. Does abstinence from ejaculation before prostate MRI improve evaluation of the seminal vesicles? *AJR Am J Roentgenol* 2016;**207**(6):1205–9.
24. Slough RA, Caglic I, Hansen NL, et al. Effect of hyoscine butylbromide on prostate multiparametric MRI anatomical and functional image quality. *Clin Radiol* 2018;**73**(2). 216.e9-216.e14.
25. Ullrich T, Quentin M, Schmaltz AK, et al. Hyoscine butylbromide significantly decreases motion artefacts and allows better delineation of anatomic structures in mp-MRI of the prostate. *Eur Radiol* 2018;**28**(1):17–23.
26. van Griethuysen JJM, Bus EM, Hauptmann M, et al. Gas-induced susceptibility artefacts on diffusion-weighted MRI of the rectum at 1.5 T—effect of applying a micro-enema to improve image quality. *Eur J Radiol* 2018;**99**:131e7.

27. Caglic I, Hansen NL, Slough RA, et al. Evaluating the effect of rectal distension on prostate multiparametric MRI image quality. *Eur J Radiol* 2017;**90**:174–80.
28. Lim C, Quon J, McInnes M, et al. Does a cleansing enema improve image quality of 3T surface coil multiparametric prostate MRI? *J Magn Reson Imaging* 2015;**42**:689e97.
29. Brizmohun Appayya M, Adshead J, Ahmed HU, et al. National implementation of multi-parametric magnetic resonance imaging for prostate cancer detection — recommendations from a UK consensus meeting. *BJU Int* 2018;**122**(1):13–25.
30. Caglic I, Barrett T. Optimising prostate mpMRI: prepare for success. *Clin Radiol* 2019 Jan 2;(18):30614–7. pii: S0009-9260.
31. Trivedi H, Turkbey B, Rastinehad AR, et al. Use of patient-specific MRI-based prostate mold for validation of multiparametric MRI in localization of prostate cancer. *Urology* 2012;**79**(1):233–9.
32. Le Bihan D, Breton E, Lallemand D, et al. Separation of diffusion and perfusion in intravoxel incoherent motion MR imaging. *Radiology* 1988;**168**:497–505.
33. Peng Y, Jiang Y, Antic T, et al. Apparent diffusion coefficient for prostate cancer imaging: impact of b values. *AJR Am J Roentgenol* 2014;**202**(3):W247–53.
34. Barrett T, Priest AN, Lawrence EM, et al. Ratio of tumor to normal prostate tissue apparent diffusion coefficient as a method for quantifying DWI of the prostate. *AJR Am J Roentgenol* 2015;**205**(6):W585–93.
35. Jensen JH, Helpert JA, Ramani A, et al. Diffusional kurtosis imaging: the quantification of non-Gaussian water diffusion by means of magnetic resonance imaging. *Magn Reson Med* 2005;**53**(6):1432–40.
36. Lawrence EM, Warren AY, Priest AN, et al. Evaluating prostate cancer using fractional tissue composition of radical prostatectomy specimens and pre-operative diffusional kurtosis magnetic resonance imaging. *PLoS One* 2016;**11**(7):e0159652.
37. Rosenkrantz AB, Sigmund EE, Johnson G, et al. Prostate cancer: feasibility and preliminary experience of a diffusional kurtosis model for detection and assessment of aggressiveness of peripheral zone cancer. *Radiology* 2012;**264**(1):126–35.
38. Panebianco V, Giganti F, Kitzing YX, et al. An update of pitfalls in prostate mpMRI: a practical approach through the lens of PI-RADS v. 2 guidelines. *Insights Imaging* 2018;**9**(1):87–101.
39. Othman AE, Falkner F, Weiss J, et al. Effect of temporal resolution on diagnostic performance of T2-weighted MRI and an apparent diffusion coefficient map. *AJR Am J Roentgenol* 2015;**205**(2):W185–92.
40. Ream JM, Doshi AM, Dunst, et al. Dynamic contrast-enhanced MRI of the prostate: an intraindividual assessment of the effect of temporal resolution on qualitative detection and quantitative analysis of histopathologically proven prostate cancer. *J Magn Reson Imag* 2016;**45**:1464. e75.
41. De Visschere P, Lumen N, Ost P, et al. Dynamic contrast-enhanced imaging has limited added value over T2-weighted imaging and diffusion-weighted imaging when using PI-RADSV2 for diagnosis of clinically significant prostate cancer in patients with elevated PSA. *Clin Radiol* 2017;**72**(1):23–32.
42. Vargas HA, Hötter AM, Goldman DA, et al. Updated prostate imaging reporting and data system (PI-RADS v2) recommendations for the detection of clinically significant prostate cancer using multiparametric MRI: critical evaluation using whole-mount pathology as standard of reference. *Eur Radiol* 2016;**26**(6):1606–12.
43. Burn PR, Freeman SJ, Andreou A, et al. A multi-centre assessment of prostate MRI quality and compliance with UK and international standards. *Clin Radiol* 2019;**74**:894.e19–25.
44. Wassberg C, Akin O, Vargas HA, et al. The incremental value of contrast-enhanced MRI in the detection of biopsy-proven local recurrence of prostate cancer after radical prostatectomy: effect of reader experience. *AJR Am J Roentgenol* 2012;**199**(2):360–6.
45. Prostate Cancer UK. mpMRI before biopsy can radically improve diagnosis. <https://prostatecanceruk.org/about-us/what-we-think-and-do/mpmri>. [Accessed 2 April 2019].
46. Moldovan PC, Van den Broeck T, Sylvester R, et al. What is the negative predictive value of multiparametric magnetic resonance imaging in excluding prostate cancer at biopsy? A systematic review and meta-analysis from the European Association of Urology Prostate Cancer Guidelines Panel. *Eur Urol* 2017;**72**(2):250–66.
47. Woo S, Suh CH, Kim SY, et al. Diagnostic performance of Prostate Imaging Reporting and Data System version 2 for detection of prostate cancer: a systematic review and diagnostic meta-analysis. *Eur Urol* 2017;**72**(2):177–88.
48. Iwazawa J, Mitani T, Sassa S, et al. Prostate cancer detection with MRI: is dynamic contrast-enhanced imaging necessary in addition to diffusion-weighted imaging? *Diagn Interv Radiol* 2011;**17**(3):243–8.
49. Krishna S, McInnes M, Lim C, et al. Comparison of prostate imaging reporting and data system versions 1 and 2 for the detection of peripheral zone Gleason score 3 + 4 = 7 cancers. *AJR Am J Roentgenol* 2017;**209**(6):W365–73.
50. Choi MH, Lee YJ, Jung SE, et al. Prebiopsy biparametric MRI: differences of PI-RADS version 2 in patients with different PSA levels. *Clin Radiol* 2018;**73**(9):810–7.
51. Quick CM, Gokden N, Sangoi AR, et al. The distribution of PAX-2 immunoreactivity in the prostate gland, seminal vesicle, and ejaculatory duct: comparison with prostatic adenocarcinoma and discussion of prostatic zonal embryogenesis. *Hum Pathol* 2010;**41**(8):1145–9.
52. Vargas HA, Akin O, Franiel T, et al. Normal central zone of the prostate and central zone involvement by prostate cancer: clinical and MR imaging implications. *Radiology* 2012;**262**(3):894–902.
53. Hansford BG, Karademir I, Peng Y, et al. Dynamic contrast-enhanced MR imaging features of the normal central zone of the prostate. *Acad Radiol* 2014;**21**(5):569–77.
54. McNeal JE. Regional morphology and pathology of the prostate. *Am J Clin Pathol* 1968;**49**(3):347–57.
55. Gupta RT, Kauffman CR, Garcia-Reyes K, et al. Apparent diffusion coefficient values of the benign central zone of the prostate: comparison with low- and high-grade prostate cancer. *AJR Am J Roentgenol* 2015;**205**(2):331–6.
56. Cohen RJ, Shannon BA, Phillips M, et al. Central zone carcinoma of the prostate gland: a distinct tumor type with poor prognostic features. *J Urol* 2008;**179**(5):1762–7.
57. Bouyé S, Potiron E, Puech P, et al. Transition zone and anterior stromal prostate cancers: zone of origin and intraprostatic patterns of spread at histopathology. *Prostate* 2009;**69**(1):105–13.
58. Ward E, Baad M, Peng Y, et al. Multi-parametric MR imaging of the anterior fibromuscular stroma and its differentiation from prostate cancer. *Abdom Radiol (NY)* 2017;**42**(3):926–34.
59. Shinmoto H, Tamura C, Soga S, et al. Anterior prostate cancer: diagnostic performance of T2-weighted MRI and an apparent diffusion coefficient map. *AJR Am J Roentgenol* 2015;**205**(2):W185–92.
60. Hansen NL, Koo BC, Warren AY, et al. Sub-differentiating equivocal PI-RADS-3 lesions in multiparametric magnetic resonance imaging of the prostate to improve cancer detection. *Eur J Radiol* 2017;**95**:307–31.
61. Chesnais AL, Niaf E, Bratan F, et al. Differentiation of transitional zone prostate cancer from benign hyperplasia nodules: evaluation of discriminant criteria at multiparametric MRI. *Clin Radiol* 2013;**68**:e323–30.
62. Søndergaard G, Vetner M, Christensen PO. Periferical cystic hyperplasia of the prostate gland. *Acta Pathol Microbiol Immunol Scand A* 1987;**95**(3):137–9.
63. Magnetta MJ, Donovan AL, Jacobs BL, et al. Evidence-based reporting: a method to optimize prostate MRI communications with referring physicians. *AJR Am J Roentgenol* 2018 Jan;**210**(1):108–12.
64. Shaish H, Feltus W, Steinman J, et al. Impact of a structured reporting template on adherence to Prostate Imaging Reporting and Data System Version 2 and on the diagnostic performance of prostate MRI for clinically significant prostate cancer. *J Am Coll Radiol* 2018;**15**(5):749–54.
65. Benndorf M, Hahn F, Krönig M, et al. Diagnostic performance and reproducibility of T2w based and diffusion weighted imaging (DWI) based PI-RADSV2 lexicon descriptors for prostate MRI. *Eur J Radiol* 2017;**93**:9–15.
66. Hansen NL, Barrett T, Koo B, et al. The influence of prostate-specific antigen density on positive and negative predictive values of multiparametric magnetic resonance imaging to detect Gleason score 7–10 prostate cancer in a repeat biopsy setting. *BJU Int* 2017;**119**(5):724–30.
67. Bhat NR, Vetter JM, Andriole GL, et al. Magnetic resonance imaging-defined prostate-specific antigen density significantly improves the risk prediction for clinically significant prostate cancer on biopsy. *Urology* 2018 Dec 20;(18). 31324-4pii: S0090-4295.
68. Panebianco V, Barchetti G, Simone G, et al. Negative multiparametric magnetic resonance imaging for prostate cancer: what's next? *Eur Urol* 2018 Jul;**74**(1):48–54.
69. Greer MD, Shih JH, Barrett T, et al. All over the map: an interobserver agreement study of tumor location based on the PI-RADSV2 sector map. *J Magn Reson Imaging* 2018;**48**(2):482–90.